



Targeting Hyaluronan Interactions for Glioblastoma Stem Cell Therapy

Joline S. Hartheimer¹ · Seungjo Park¹ · Shreyas S. Rao¹ · Yonghyun Kim¹

Received: 25 January 2019 / Accepted: 16 April 2019 / Published online: 11 May 2019
© Springer Nature B.V. 2019

Abstract

Even with rigorous treatments, glioblastoma multiforme (GBM) has an abysmal median survival rate, greatly due to the drug-resistant glioblastoma stem cell (GSC) population. GSCs are known to remodel their microenvironment, but the precise role of extracellular matrix components hyaluronic acid (HA) and hyaluronidases (HAases) on the GSC population is still largely unknown. Our objective was to determine how HAase can sensitize GSCs to chemotherapy drugs by disrupting the HA-CD44 signaling. GBM cell line U87-MG and patient-derived D456 cells were grown in GSC-enriching media and treated with HA or HAase. Expressions of GSC markers, HA-related genes, and drug resistance genes were measured via flow cytometry, confocal microscopy, and qRT-PCR. Proliferation after combined HAase and temozolomide (TMZ) treatment was measured via WST-8. HA supplementation promoted the expression of GSC markers and CD44 in GBM cells cultured in serum-free media. Conversely, HAase addition inhibited GSC gene expression while promoting CD44 expression. Finally, HAase sensitized GBM cells to TMZ. We propose a combined treatment of HAase and chemotherapy drugs by disrupting the stemness-promoting HA to target GSCs. This combination therapy shows promise even when temozolomide treatment alone causes resistance.

Keywords Glioblastoma (GBM) · Hyaluronic acid (HA) · Tumor microenvironment · Temozolomide (TMZ) · Combination therapy

Introduction

Glioblastoma multiforme (GBM) is the deadliest form of brain cancer with an abysmal median progression-free survival rate of 10.6 months, despite aggressive treatments such as radiotherapy, anti-angiogenic treatments (e.g., bevacizumab), and DNA alkylating agents such as temozolomide [1]. The glioblastoma stem cell (GSC) subpopulation has been identified to have self-renewal capacity and resistance to currently available GBM treatments. For example, CD133+ GSCs were found to survive high-dose radiation therapy and accumulate in remnant tumors after resection [2]. GSCs are

also thought to contribute to chemoresistance through the induction of autophagy, apoptosis, and the unfolded protein response by temozolomide (TMZ) [3]. The ineffectiveness of current GBM treatments can therefore be attributed to their failure to adequately target GSCs.

The tumor microenvironment plays a key role in controlling the fate of GBM cells. For example, GBM migration, chemoresistance, and stemness have been found to be strongly dependent on the extracellular matrix (ECM) composition [4–6]. Hyaluronan (HA) is the main component of the brain ECM, particularly in the white matter tracts that support glioma invasion, and GSCs interact with HA in their microenvironment via receptors CD44 and RHAMM [7]. HA metabolism in the ECM is controlled by HA synthases (HAS) and hyaluronidases (HAases), and HA-CD44 signaling has been found to promote cancer cell proliferation, invasion, and chemoresistance [8, 9]. HA's role in protecting cancer cells from chemotherapy therefore makes it an attractive molecule for targeted therapy.

Normal proliferating cells shed their HA coat via the action of HAase, and the failure to lose this coat is implicated in cancer development. Higher HA levels were correlated with

Electronic supplementary material The online version of this article (<https://doi.org/10.1007/s12307-019-00224-2>) contains supplementary material, which is available to authorized users.

✉ Yonghyun Kim
ykim@eng.ua.edu

¹ Department of Chemical and Biological Engineering, The University of Alabama, Box 870203, Tuscaloosa, AL 35487-0203, USA

worse prognosis, and cancer cells were found to induce HA production in surrounding stromal cells [10]. Cancer cells are known to actively remodel their microenvironment, manipulating the mosaic of differently sized HA molecules in the brain to suit their unique migration and invasion patterns. Since HAases break down polymeric HA, they have been found to improve physical drug delivery with HA depletion lowering tumor interstitial pressure, increasing perfusion, and reversing hypoxia [11, 12]. PH20, the human recombinant form of HAase, improved viral spreading of an oncolytic virus in GBM, and phase II and III clinical trials of PH20 plus chemotherapy in metastatic pancreatic ductal adenocarcinoma are currently underway [13, 14].

While HAases appear to successfully overcome physical drug delivery barriers in cancer, it is unknown how HAases specifically interact with GSCs. We hypothesized that HAase would sensitize GSCs to chemotherapeutics by inhibiting HA-CD44 signaling that promotes stemness. To test this hypothesis, we studied the effect of both HA and HAase on U87-MG and patient-derived GBM D456 cells enriched for GSCs. We also investigated the impact of combining HAase and TMZ treatment on proliferation.

Methods

Glioblastoma Bio Discovery Portal

The multi-gene prognostic index for a group of HA-related genes (HAS1, HAS2, RHAMM, and CD44) was analyzed by GBM molecular subtype using the National Cancer Institute's Glioblastoma Bio Discovery Portal software (GBM Bio-DP; <https://gbm-biodp.nci.nih.gov>), which accesses and visualizes data from The Cancer Genome Atlas (TCGA) [15]. 197 samples were analyzed using Cox proportional hazards model. Each sample's prognostic index was determined by averaging individual gene expression from the Cox regression coefficient. Prognostic index was stratified into highest and lowest expression quartiles for both the entire cohort and each molecular subtype: classical, mesenchymal, proneural, and neural [16].

Cell Culture

Two glioblastoma cell types were used: U87-MG cell line (ATCC, Manassas, VA) and D456 glioblastoma cells. D456 is a proneural subtype patient-derived xenograft GBM line kindly provided by Dr. G. Yancey Gillespie (Department of Neurosurgery, University of Alabama at Birmingham) and originally established by Dr. Darrell Bigner (Duke University Medical Center). D456 is derived from a human

pediatric fronto-parietal GBM directly implanted into the flank of immunocompromised mice, as previously described [17].

Both cell types were grown in either GSC-enriching sphere culture media NBE or serum containing adherent culture media MEM (for HAase-TMZ experiments) at 37 °C in a 5% CO₂ environment. NBE consists of Neurobasal-A media (Gibco) supplemented with 1 mM L-glutamine (Gibco), 8 µg/mL heparin (Akron biotechnology), 0.5X B27 (Gibco), 1% Penicillin/Streptomycin (Corning), 20 ng/mL EGF (Shenandoah Biotechnology), and 20 ng/mL bFGF (Shenandoah Biotechnology). MEM is minimum essential media (Gibco) supplemented with 10% fetal bovine serum (Gibco) and 1% Penicillin/Streptomycin (Corning).

HA and HAase Treatment

For HA treatment, both U87-MG and D456 cells were treated with 60 kDa sodium hyaluronate (Lifecore Biomedical) at various concentrations (i.e., 0, 20, 100, or 200 µg/mL). Cells were grown in 6-well plates with 3 mL NBE media per well and treated for a full passage length: 6 days for U87-MG and 5 days for D456 cells. For HAase treatment, both U87-MG and D456 cells were treated with HAase from bovine testes Type 1-S lyophilized powder, 400–1000 units/mg solid (Sigma) suspended in PBS at various concentrations (i.e., 0, 15, or 30 U/mL). Cells were grown in NBE media in 6-well plates for a full passage length.

Extreme Limiting Dilution Analysis (ELDA)

As a functional measure of stemness after HA treatment, U87-MG and D456 cells were seeded at 1, 2, 3, 5, and 10 cells/well in 96-well plates containing 100 µL of NBE media (0 µg/mL HA or 100 µg/mL HA) per well ($n = 16$ wells per seeding density and media condition). On day 14, the number of wells containing spheres were counted, with a sphere defined as a cell aggregate of 50 µm diameter or larger. Analysis was conducted using the ELDA software from the Walter+Eliza Hall Bioinformatics Institute of Medical Research [18].

Flow Cytometry

To measure SOX2- and CD44-positive populations via flow cytometry, U87-MG and D456 cells were cultured in NBE with varying concentrations of HA for a full passage. For SOX2 measurement, cell pellets were fixed and permeabilized with BD Cytofix/Cytoperm™ solution (BD) and BD Perm/Wash buffer (BD). Pellets were then stained with rabbit anti-SOX2 IgG polyclonal primary antibody (Proteintech) and goat anti-rabbit IgG Alexa Fluor 488 polyclonal secondary

antibody (EMD Millipore). For CD44 measurement, cell pellets were stained with mouse anti-human IgG_{2b, κ} CD44 APC conjugated antibody (BD Pharmingen™). Flow cytometry was performed with BD Accuri™ C6 Flow Cytometer.

Microscopy

Cell culture brightfield micrographs were obtained with VWR VistaVision microscope. Confocal microscopy was used to qualitatively examine baseline protein-level expressions of NANOG, SOX2, and HYAL1 in D456 cells cultured in NBE. Cell pellets were flash frozen in liquid nitrogen and fixed and permeabilized with BD Cytfix/Cytoperm™ solution (BD) and BD Perm/Wash buffer (BD). All cells were stained with DAPI (Invitrogen) and respective antibodies. Cells were stained with mouse anti-human IgG_{1, κ} NANOG PE conjugated antibody (BD), mouse anti-SOX2 IgG_{1, κ} Alexa Fluor 647 conjugated antibody (BD), or mouse anti-HYAL1 IgG₁ monoclonal primary antibody (Santa Cruz Biotechnology) and rat anti-mouse IgG₁ APC secondary antibody (BD). All images were obtained with Leica TCS SP2 AOBs Confocal Microscope with 4% laser power at the University of Alabama Optical Analysis Facility.

Quantitative Reverse Transcription Polymerase Chain Reaction (qRT-PCR)

Primers were designed by retrieving nucleotide sequences from NCBI gene database for *SOX2*, *NANOG*, *CD133*, *NES*, *OCT4*, *CD44*, *RHAMM*, *HAS2*, *HYAL1*, *HYAL2*, *MDR1*, *EGFR*, and *STAT3*. Primer sequences are described in Supplementary Table 1. Primers were synthesized by Invitrogen.

The GeneJet RNA Purification kit (Thermo Scientific) was used for RNA isolation and RNA was quantified using Qubit 2.0 fluorometer (Life Technologies-Invitrogen, Carlsbad, CA, USA) and Qubit RNA HS Assay Kit (Invitrogen), or NanoVue Plus spectrophotometer (Biochrom, Holliston, MA). cDNA was synthesized using qScript cDNA SuperMix (Quanta Biosciences) and Mastercycler Nexus Gradient Thermal Cycler (Eppendorf, Hauppauge, NY). Real-time PCR was performed using PowerUp SYBR Green Master Mix (Applied Biosystems) and the StepOnePlus Real-time PCR System (Applied Biosystems). StepOne Software (v2.3) was used for the data analysis with the $\Delta\Delta C_t$ method.

Combined HAase-TMZ Treatment and Proliferation Assay

Combined HAase-TMZ treatment was performed in a 96-well plate. 5000 U87-MG or D456 cells were seeded per well in 100 μ L NBE or MEM and cultured for 72 h prior to treatment

to allow for NBE samples to form small tumorspheres and MEM samples to become confluent. At 72 h, cells were treated with varying concentrations of HAase (0 U/mL, 15 U/mL, or 100 U/mL) and temozolomide (400 μ M for U87-MG and 200 μ M for D456) (TMZ; Enzo ALX-420-044-M025) dissolved in DMSO (VWR International). Control wells were treated with DMSO and PBS, and media-only cell-free wells were used for OD value normalization. Cells were treated with HAase-TMZ for 48 h, at which time a WST-8 assay was performed according to manufacturer's protocol.

Statistical Analyses

All experiments were performed with at least triplicates for each condition. Data were analyzed using a 2-tailed t-test with equal or unequal variance and ANOVA. F-test was used to determine variance prior to t-test or ANOVA. *P*-values less than 0.05 were considered significant.

Results

HA-Related Gene Expression in GBM is Correlated with Decreased Survival

The TCGA Bio-DP was used to compare the effects of HA-related gene expression on prognostic index of large dataset of GBM patient samples using the Cox model. The highest quartile multi-gene expression of the group of HA-related genes HAS1, HAS2, CD44, and RHAMM was found to be significantly correlated with decreased prognostic index, while the lowest quartile expression of these HA-promoting genes was significantly correlated with increased prognostic index (Fig. 1a). When the patient samples were divided into molecular subtype, classical, proneural, and neural subtypes were found to have significant hazard ratios (Fig. 1b). This analysis of existing GBM patient datasets emphasizes the importance of targeting HA-interactions in GBM in order to design more effective therapeutics.

GSC Markers, HA Receptors, and Drug Resistance Genes are Highly Co-expressed in GBM

Expressions of GSC marker SOX2 and HA-receptor CD44 were measured for U87-MG and D456 cells grown in NBE using flow cytometry. Over 80% of both cell types expressed both markers with or without soluble HA addition (Fig. 2a). This established a large GSC population in both cells, as well as the potential to target HA-CD44 interactions. Confocal microscopy was also performed on dissociated D456 spheres and we found that GSC markers NANOG and SOX2 were very highly

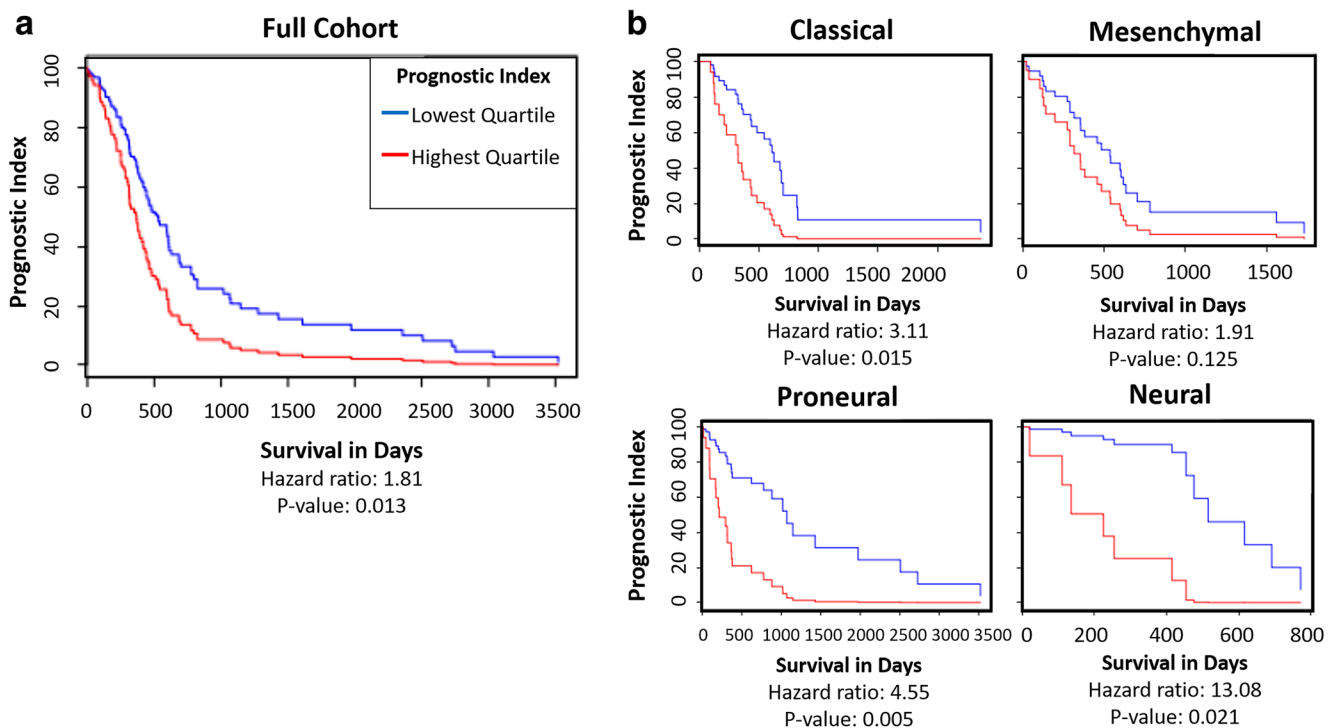


Fig. 1 TCGA GBM datasets show that higher expression of HA-related genes is correlated with lower survival rates. **a** Prognostic Index for HAS1, HAS2, RHAMM, and CD44 gene group, lowest quartile expression compared to highest quartile expression. Multi-gene prognostic

indexes and hazard ratios determined with Cox model. **b** Prognostic Index for HAS1, HAS2, RHAMM, and CD44 gene group divided by GBM molecular subtypes

expressed, while hyaluronidase gene *HYAL1* had low expression (Fig. 2b). Baseline gene expression of GSC markers, HA-related genes, and drug resistance markers was compared between the cell types via qRT-PCR (Fig. 2c). U87-MG was found to have significantly higher *NES*, *RHAMM*, and *EGFR* expression, while D456 had higher *NANOG* expression. In general, U87-MG had higher drug resistance gene expression, which suggests that it would be more resistant to chemotherapy drugs, potentially through its HA-CD44 interactions. *MDR1* was not detected in D456 cells, suggesting it may show increased chemosensitivity compared to U87-MG cells.

HA Promotes GSC Sphere Formation

When GBM cells were treated with increasing concentrations of soluble HA, there was a noted increase in sphere size in both U87-MG and D456; however, spheres remained quite heterogeneous in size and shape (Fig. 3a). Since neurosphere formation is a key functional characteristic of GSCs [19], our results indicate that HA enhances the GSC microenvironment. We also quantitatively assayed how HA treatment affects gene expression of HAases, GSC markers, and the HA receptor

CD44 using qRT-PCR (Fig. 3b). We found that 100 $\mu\text{g}/\text{mL}$ of HA increases GSC markers, *HYAL2*, and *CD44* in U87-MG cells. In addition, HA significantly promoted *NANOG* expression in both cell lines, whereas *NES*, *CD133* (*PROM1*), were enhanced only in U87-MG cells. Of particular note is that U87-MG cells had relatively low baseline *NANOG* expression in comparison to D456, but with HA addition increased its expression 5-fold. Since *CD44* was also upregulated with HA treatment, we propose that HA is maintaining the GSC microenvironment through signaling with CD44. In order to exclude that HA is impacting cell aggregation rather than sphere formation, we tested for clonogenicity using ELDA with and without 100 $\mu\text{g}/\text{mL}$ HA treatment. HA either improved the sphere forming ability (i.e., clonogenicity) for U87-MG, with a significant difference in stem cell frequency between HA-treated and non-HA-treated cells (Fig. 3c). D456 similarly showed higher sphere forming ability upon treatment with HA (steeper slope in Fig. 3c), albeit not at statistically significant levels. Stronger sphere forming ability is a sign of higher self-renewal, a key property of GSCs, and non-stem GBM cells have been shown to acquire increased self-renewal capacity upon TMZ treatment measured via

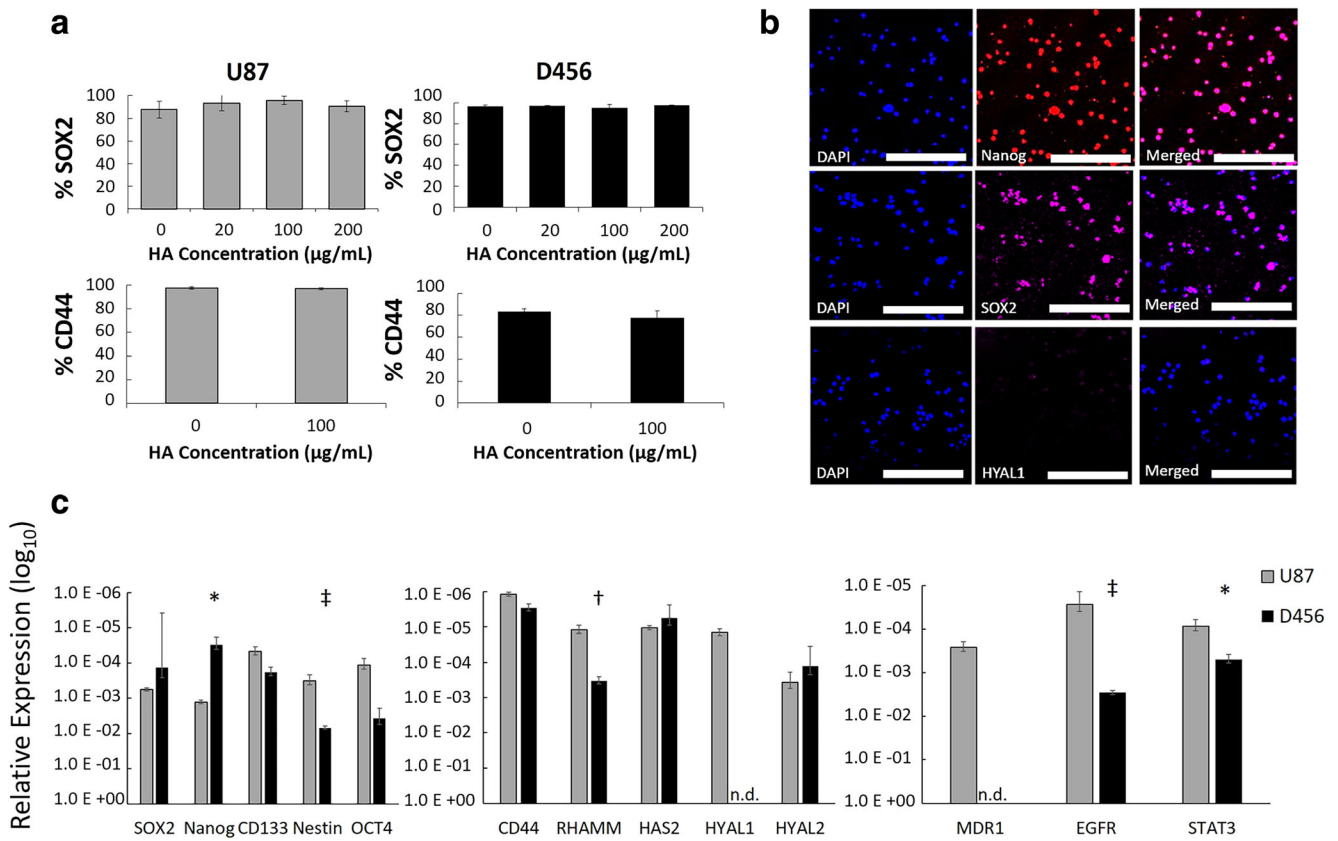


Fig. 2 At baseline, GSC markers, HA receptors, and drug resistance genes are highly co-expressed in GBM, with cell-line dependence. **a** Percent of population expressing SOX2 and CD44 within U87-MG and D456 cells treated in NBE with varying concentrations of HA for a full passage length, measured via flow cytometry (mean ± SE; $n = 3$). **b** Confocal microscopy was performed on D456 cells grown in NBE for NANOG, SOX2, and HYAL1 (scale bars = 200 µm). **c** qRT-PCR gene

expression of (left to right) GSC markers, HA-related genes, and drug resistance genes in U87-MG and D456 cells. Reported as relative expression compared to housekeeping gene GAPDH with log₁₀ transformation and significance noted between cell lines. HYAL1 and MDR1 were lower than detection level (n.d.) in D456 (mean ± SE; $n = 3$; * $p < 0.05$, † $p < 0.01$, and ‡ $p < 0.001$)

ELDA [20]. These data indicate that intermediate molecular weight HA in the brain microenvironment supports the GSC population in U87-MG and D456 cells.

HAase Causes Differentiated Phenotype and Decreased Proliferation in U87-MG Cells

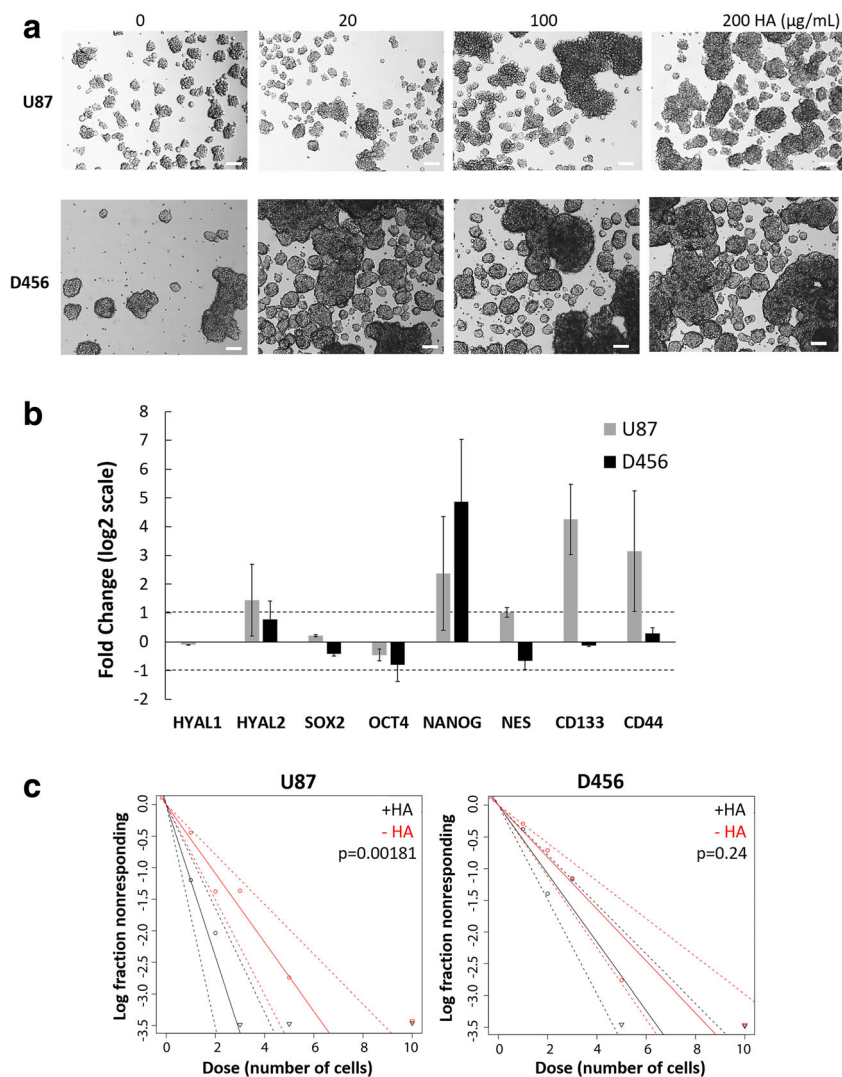
Since we found that HA is involved in preserving the GSC population, we hypothesized that HAase could disrupt the GSC microenvironment through interrupting HA-CD44 signaling. We tested this by treating U87-MG and D456 cells with varying concentrations of HAase. We found that HAase treatment resulted in an adherent morphology consistent with a differentiated phenotype in U87-MG cells, as well as notable breakdown of spheres into single cells (Fig. 4a). However, these changes were not seen in micrographs of D456 cells, presumably due to its denser and tighter spheres resisting the effects of HAase on cell-cell interactions. HAase also caused

significantly decreased cell proliferation in U87-MG cells at the 30 U/mL concentration, but did not have significant growth effects on D456 cells (Fig. 4b). These data suggest that in U87-MG cells, HAase promotes an adherent, differentiated phenotype and inhibits proliferation.

HAase Decreases Stemness Through CD44-Mediated Signaling

To assess the effects of HAase on GSCs at the genotypic level, we performed qRT-PCR on U87-MG and D456 cells treated with HAase for a full passage. We tested for stemness markers *CD133*, *SOX2*, *NES*, and *NANOG*, and found that HAase caused a significant decrease in *SOX2* for U87-MG and *CD133* for D456 cells (Fig. 5a). To determine the route of HAase’s impact on stemness, we measured expression of HA-related genes *HAS2*, *RHAMM*, and *CD44* (Fig. 5b). In both cell lines, there was a significant increase in HA-

Fig. 3 HA promotes GSC sphere formation. **a** Representative micrographs of U87-MG and D456 cells treated with HA for a full passage length (scale bar = 100 μ m). **b** qRT-PCR gene expression of U87-MG and D456 cells treated with HA for a full passage length. Represented as fold change compared to control cells. *HYAL1* was not detected in D456 cells. The \log_2 transforms of fold changes greater than 1 or less than 1 were considered significant (mean \pm SE; $n = 3$). **c** ELDA of U87-MG and D456 cells treated without (“-HA”) or with HA (100 μ g/mL; “+HA”) for 14 days (dotted lines 95% CI; $n = 16$; $p < 0.05$ indicates significant change in stem cell frequency)



receptor *CD44* expression, suggesting that HAase has an inhibitory effect on stemness through *CD44*-mediated signaling. Drug resistance genes *STAT3*, *EGFR*, and *MDR1* were also tested, and U87-MG showed an unexpected significant increase in *MDR1* while D456 showed a very significant decrease in *STAT3* (Fig. 5c). The increase in *MDR1* could be explained by U87-MG's higher drug resistance gene expression at baseline and lessened impact to HAase, compared to D456. *STAT3* is regulator of gliomagenesis that is constitutively activated in GBM, and its decrease is correlated with decreased survival, invasion, angiogenesis, and immune suppression of GBM cells [21]. Overall, these data show that HAase reduces expression of GSC markers *SOX2* in U87-MG cells and *CD133* in D456 cells by *CD44*-mediated signaling, and that HAase decreases expression of the transcription factor *STAT3* in D456 cells.

HAase is Cytotoxic to GBM Cells and Increases TMZ Sensitivity in GSC-Promoting Culture

To examine the impact of HAase combined with chemotherapy drugs, we measured proliferation of GBM cells treated with TMZ and/or HAase via WST-8. Both 200 μ M and 400 μ M concentrations of TMZ were tested on U87-MG cells, and due to a higher drug resistance of U87-MG to TMZ, 400 μ M was chosen as the most appropriate concentration for further studies. D456 cells were sensitive to TMZ at 200 μ M, so that concentration was used. We found that after 48 h of treatment, U87-MG cells grown in serum-containing media showed a cytotoxic effect of HAase alone but no significant effects when HAase was combined with TMZ (Fig. 6a). However, U87-MG cells grown in GSC-promoting NBE media showed both a cytotoxic effect of HAase alone as

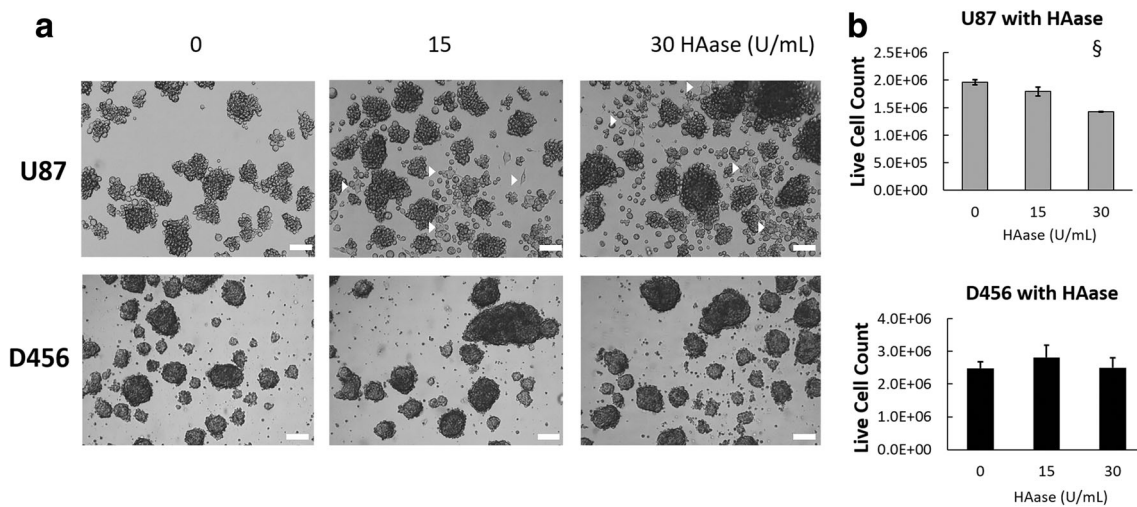


Fig. 4 HAase causes differentiated phenotype and attenuated growth in U87-MG cells, but not in D456 cells. **a** Representative micrographs of U87-MG and D456 cells treated with HAase for a full passage length. Arrowheads show adhered cells with spread morphology (scale bar =

100 μ m). **b** Live cell counts of U87-MG and D456 cells treated with HAase for a full passage length. Dead population was determined with trypan blue staining prior to automatic cell counts (mean \pm SE; $n = 3$; § $p < 0.0001$)

well as a significant combined effect with TMZ at the higher concentration 100 U/mL of HAase (Fig. 6b). Additionally, U87-MG grown in both serum and NBE showed a surprising increase in proliferation upon TMZ treatment. This may be due to TMZ causing drug resistance by converting differentiated GBM cells into highly proliferative GSCs, as has been found with TMZ primary chemotherapy in previous studies [22]. In D456 cells, there was no increased proliferative effect of TMZ alone and HAase was cytotoxic at all conditions (Fig. 6c). Additionally, a significant combined effect of HAase and TMZ at both 15 U/mL and 100 U/mL of HAase was seen for D456 cells. Overall, these data demonstrate that HAase preferentially sensitizes GSCs to TMZ.

Discussion

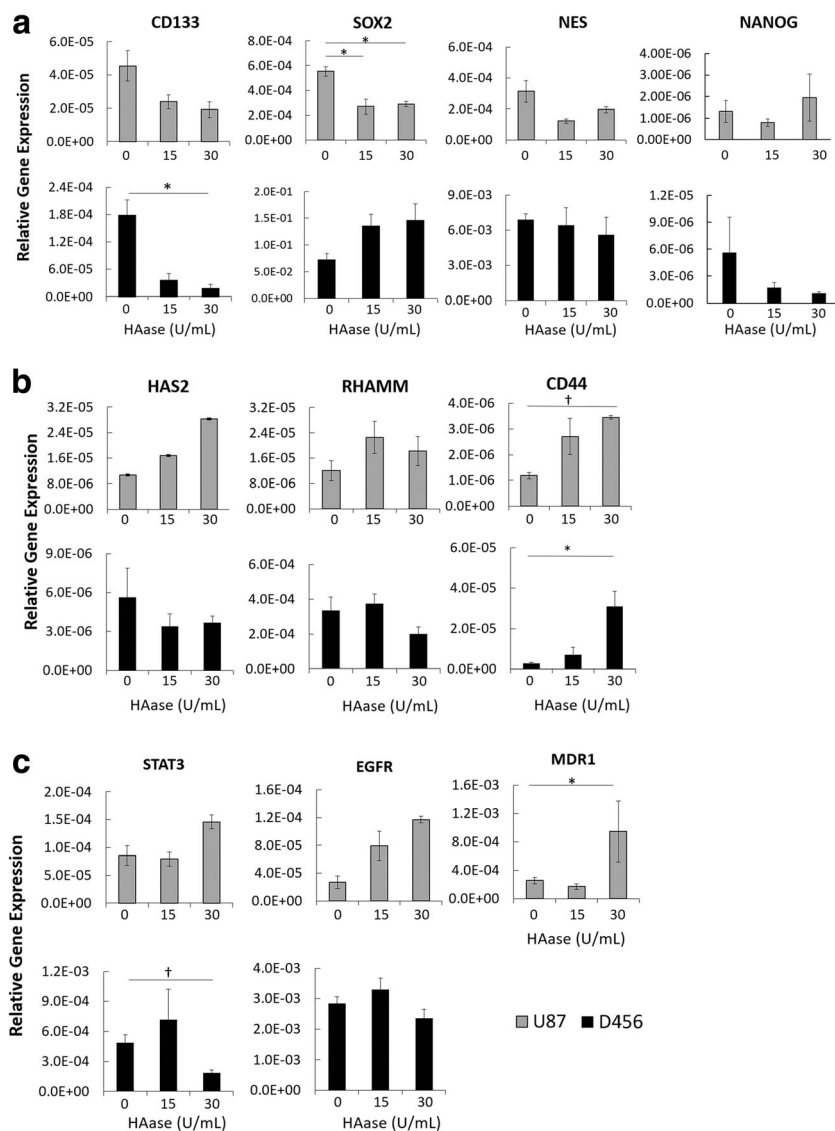
At this time, little is known about the role of HAase in GSCs. There have been contradictory studies on the roles of HYAL1 and HYAL2 in tumor progression, but these paradoxes were attributed to dose-dependent effects [23]. Even though bovine HAase has been found in the past to improve patient survival when added to chemotherapy through degrading physical drug delivery barriers and increasing drug perfusion, much of its study was halted due to the bovine HAase causing severe allergic reactions in patients [12, 24, 25]. Specifically, in an astrocytoma study, 20% of patients had allergic reactions after being treated with bovine HAase intravenously [26]. However, a new human recombinant form of HAase (HylenexTM) has been recently created that has not caused

allergic reactions and is currently being used in several clinical trials in PEGylated form [27]. This presents an opportunity to reconsider the therapeutic role of HAase in GBM, particularly on the drug-resistant GSC population.

Our data showed that HAase had a cytotoxic effect on both the established U87-MG cell line and patient-derived D456 cells grown in GSC-promoting media. When combined with TMZ, HAase had a synergistic effect only at the higher concentration of HAase (100 U/mL) for U87-MG cells, and at both low (15 U/mL) and high concentrations of HAase for D456 cells. These cell line differences can be attributed to U87-MG having significantly higher drug resistance gene expression (*EGFR* and *MDR1*) at baseline compared to D456 cells. In addition, U87-MG cells required higher doses of TMZ than D456 cells to obtain similar effects on proliferation. Therefore, D456 cells are likely more chemosensitive and responsive to the synergistic effects of HAase and TMZ than U87-MG cells.

An unexpected result was the increase in relative cell number when U87-MG was treated with TMZ alone. This could have been due to TMZ killing the non-GSC population, leaving behind only the more drug-resistant GSCs. A previous study found that TMZ failed to target the quiescent GSC-like population that sustains long-term tumor growth; the quiescent GSC-like cells are the source of highly proliferative tumor cells produced at a later time [28]. This emphasizes the importance of effective first-line chemotherapy for GBM, as improper chemotherapy regimens can increase stemness and make tumors even harder to treat. There is

Fig. 5 HAase decreases stemness through involvement of CD44 signaling. qRT-PCR gene expression of U87-MG and D456 cells treated with HAase for a full passage length. **a** GSC markers *CD133*, *SOX2*, *NES*, and *NANOG*. **b** HA-related genes *HAS2*, *RHAMM*, and *CD44*. **c** Drug resistance genes *STAT3*, *EGFR*, and *MDR1*. *MDR1* was not detected in D456 cells. All genes reported as relative expression compared to housekeeping gene *GAPDH* (mean \pm SE; $n = 3$; * $p < 0.05$, † $p < 0.01$)



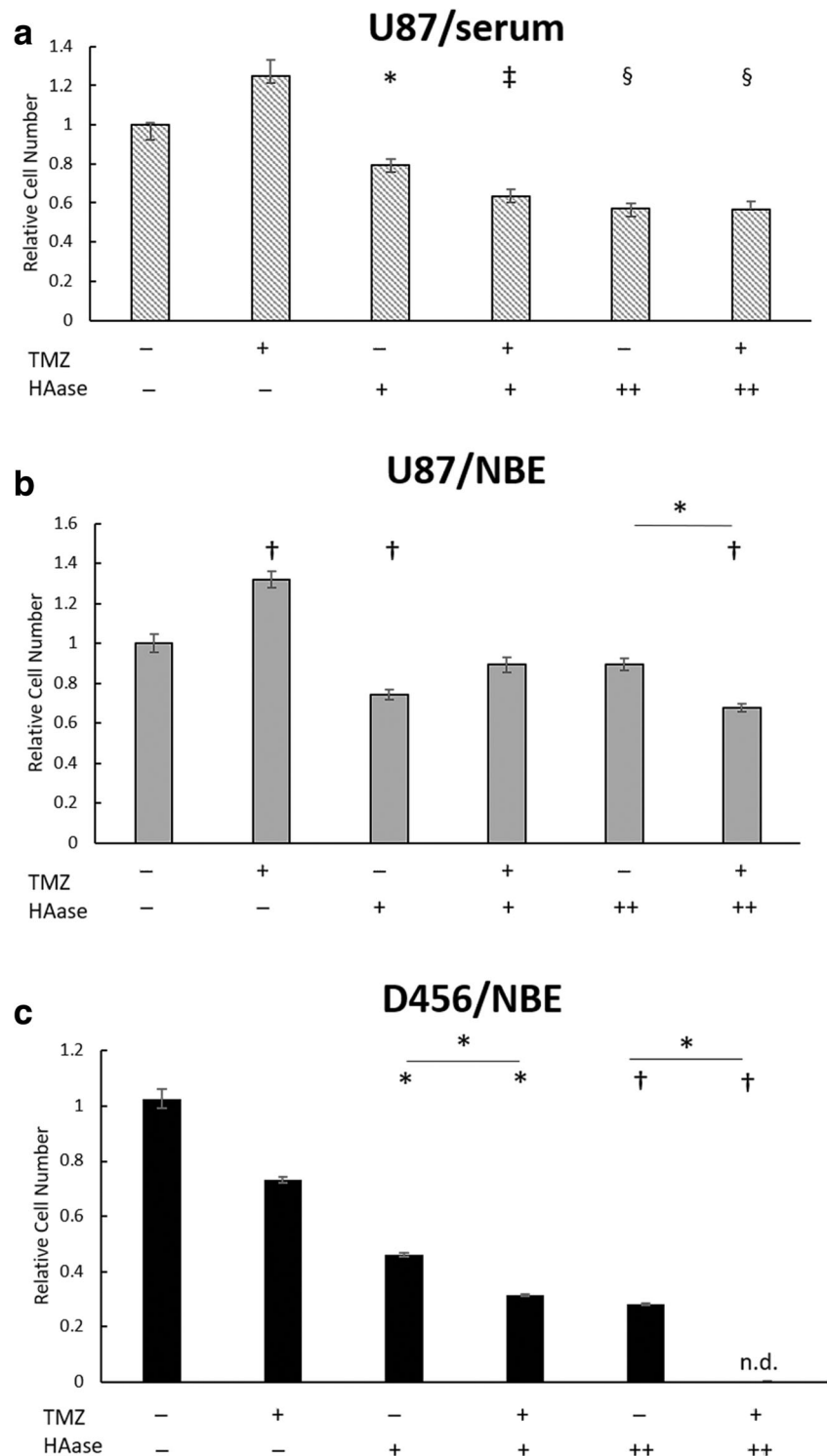
currently no standard of care for treatment of recurrent GBM and second-line chemotherapy has so far shown only discouraging results [29]. Adding HAase to drugs could allow GSCs to be targeted during early treatments to avoid recurrence.

As for the role of the HA receptor CD44 in HAase treatment, we found that HAase increased expression of *CD44* while it decreased *SOX2* for U87-MG and *CD133* for D456 cells. While *CD44* has previously been suggested to be a GSC marker itself, a recent study found that *CD44* knockdown actually increased the stemness phenotype and increased GSC markers *CD133*, *NES*, and *OCT4* [30]. This suggests that CD44 may not be an appropriate GSC marker and our observed increase in its expression did not necessarily correlate with an increase in stemness. CD44 has also been found to be essential for the catabolic function of both exogenously and endogenously expressed *HYAL1* and *HYAL2* [31].

In another study, *HYAL2* overexpression caused CD44 to lose half of its capacity to bind exogenous HA as well as decreasing cell motility, showing that HAase disrupts formation of the HA pericellular coat through interaction with CD44 [32]. Thus, in our experiments, HAase interactions with CD44 may be forcing endogenous HA to compete for CD44 interactions, and thereby inhibiting HA's ability to protect GSCs.

In summary, the combined HAase-TMZ treatment of GBM showed promise in both decreasing stemness and creating a synergistic therapeutic effect in vitro. Our data also warrant future study of HAase and chemotherapy combination treatment in vivo and in other cancers associated with accumulation of HA in the ECM, including the breast, lung, ovary, and gastrointestinal tract [33]. We anticipate our findings would be useful for developing better chemotherapy regimens to target the drug-resistant GSC population causing tumor recurrence.

Fig. 6 HAase is cytotoxic to GBM cells and increases TMZ sensitivity in GSC-promoting culture. **a** Treatment of U87-MG cells grown in MEM media containing serum (+TMZ = 400 μ M). **b** Treatment of U87-MG cells grown in GSC-promoting NBE media (+TMZ = 400 μ M). **c** Treatment of D456 cells grown in GSC-promoting NBE media (+TMZ = 200 μ M). Relative cell number was measured via a WST-8 assay after 48 h treatment with TMZ and/or HAase on Day 3 (+HAase = 15 U/mL; ++HAase = 100 U/mL). Both normalization and significance were determined relative to DMSO/PBS treated control wells (mean \pm SE; $n = 8$; * $p < 0.05$, † $p < 0.01$, ‡ $p < 0.001$, and § $p < 0.0001$)



Acknowledgements The authors would like to thank Dr. G. Yancey Gillespie (University of Alabama at Birmingham) for providing the D456 patient-derived xenograft GBM line. The authors would like to further acknowledge financial support from the National Science Foundation (CBET 1604677 to Y.K. and S.R.), the University of Alabama Randall Research Scholars Program (J.S.H.), and by the Alabama Experimental Program to Stimulate Competitive Research (S.P.). S.D.G.

References

- Chinot OL, Wick W, Mason W, Henriksson R, Saran F, Nishikawa R, Carpentier AF, Hoang-Xuan K, Kavan P, Cemea D, Brandes AA, Hilton M, Abrey L, Cloughesy T (2014) Bevacizumab plus radiotherapy-temozolomide for newly diagnosed glioblastoma. *N Engl J Med* 370:709–722. <https://doi.org/10.1056/NEJMoa1308345>
- Tamura K, Aoyagi M, Wakimoto H, Ando N, Nariai T, Yamamoto M, Ohno K (2010) Accumulation of CD133-positive glioma cells

- after high-dose irradiation by Gamma Knife surgery plus external beam radiation. *J Neurosurg* 113:310–318. <https://doi.org/10.3171/2010.2.jns091607>
3. Hombach-Klonisch S, Mehrpour M, Shojaei S, Harlos C, Pitz M, Hamai A, Siemianowicz K, Likus W, Wiechec E, Toyota BD, Hoshyar R, Seyfoori A, Sepehri Z, Ande SR, Khadem F, Akbari M, Gorman AM, Samali A, Klonisch T, Ghavami S (2018) Glioblastoma and chemoresistance to alkylating agents: involvement of apoptosis, autophagy, and unfolded protein response. *Pharmacol Ther* 184:13–41. <https://doi.org/10.1016/j.pharmthera.2017.10.017>
 4. Kimlin LC, Casagrande G, Virador VM (2013) In vitro three-dimensional (3D) models in cancer research: an update. *Mol Carcinog* 52:167–182. <https://doi.org/10.1002/mc.21844>
 5. Herrera-Perez M, Voytik-Harbin SL, Rickus JL (2015) Extracellular matrix properties regulate the migratory response of glioblastoma stem cells in three-dimensional culture. *Tissue Eng Part A* 21:2572–2582. <https://doi.org/10.1089/ten.TEA.2014.0504>
 6. Lv D, Yu SC, Ping YF, Wu H, Zhao X, Zhang H, Cui Y, Chen B, Zhang X, Dai J, Bian XW, Yao XH (2016) A three-dimensional collagen scaffold cell culture system for screening anti-glioma therapeutics. *Oncotarget* 7:56904–56914. <https://doi.org/10.18632/oncotarget.10885>
 7. Akiyama Y, Jung S, Salhia B, Lee S, Hubbard S, Taylor M, Mainprize T, Akaishi K, van Furth W, Rutka JT (2001) Hyaluronate receptors mediating glioma cell migration and proliferation. *J Neuro-Oncol* 53:115–127. <https://doi.org/10.1023/a:1012297132047>
 8. Toole BP (2009) Hyaluronan-CD44 interactions in cancer: paradoxes and possibilities. *Clin Cancer Res* 15:7462–7468. <https://doi.org/10.1158/1078-0432.CCR-09-0479>
 9. Karbownik MS, Nowak JZ (2013) Hyaluronan: towards novel anti-cancer therapeutics. *Pharmacol Rep* 65:1056–1074
 10. Stern R (2008) Association between cancer and “acid mucopolysaccharides”: an old concept comes of age, finally. *Semin Cancer Biol* 18:238–243. <https://doi.org/10.1016/j.semcancer.2008.03.014>
 11. Shepard HM (2015) Breaching the castle walls: Hyaluronan depletion as a therapeutic approach to cancer therapy. *Front Oncol* 5:192. <https://doi.org/10.3389/fonc.2015.00192>
 12. Thompson CB, Shepard HM, O'Connor PM, Kadhim S, Jiang P, Osgood RJ, Bookbinder LH, Li X, Sugarman BJ, Connor RJ, Nadjsombati S, Frost GI (2010) Enzymatic depletion of tumor hyaluronan induces antitumor responses in preclinical animal models. *Mol Cancer Ther* 9:3052–3064. <https://doi.org/10.1158/1535-7163.MCT-10-0470>
 13. Guedan S, Rojas JJ, Gros A, Mercade E, Cascallo M, Alemany R (2010) Hyaluronidase expression by an oncolytic adenovirus enhances its intratumoral spread and suppresses tumor growth. *Mol Ther* 18:1275–1283. <https://doi.org/10.1038/mt.2010.79>
 14. Wong KM, Horton KJ, Covelev AL, Hingorani SR, Harris WP (2017) Targeting the tumor stroma: the biology and clinical development of Pegylated recombinant human hyaluronidase (PEGPH20). *Curr Oncol Rep* 19:47. <https://doi.org/10.1007/s11912-017-0608-3>
 15. Celiku O, Johnson S, Zhao S, Camphausen K, Shankavaram U (2014) Visualizing molecular profiles of glioblastoma with GBM-BioDP. *PLoS One* 9:e101239. <https://doi.org/10.1371/journal.pone.0101239>
 16. Verhaak RG, Hoadley KA, Purdom E, Wang V, Qi Y, Wilkerson MD, Miller CR, Ding L, Golub T, Mesirov JP, Alexe G, Lawrence M, O'Kelly M, Tamayo P, Weir BA, Gabriel S, Winckler W, Gupta S, Jakkula L, Feiler HS, Hodgson JG, James CD, Sarkaria JN, Brennan C, Kahn A, Spellman PT, Wilson RK, Speed TP, Gray JW, Meyerson M, Getz G, Perou CM, Hayes DN, Cancer Genome Atlas Research N (2010) Integrated genomic analysis identifies clinically relevant subtypes of glioblastoma characterized by abnormalities in PDGFRA, IDH1, EGFR, and NF1. *Cancer Cell* 17:98–110. <https://doi.org/10.1016/j.ccr.2009.12.020>
 17. Friedman GK, Langford CP, Coleman JM, Cassady KA, Parker JN, Markert JM, Yancey Gillespie G (2009) Engineered herpes simplex viruses efficiently infect and kill CD133+ human glioma xenograft cells that express CD111. *J Neuro-Oncol* 95:199–209. <https://doi.org/10.1007/s11060-009-9926-0>
 18. Hu Y, Smyth GK (2009) ELDA: extreme limiting dilution analysis for comparing depleted and enriched populations in stem cell and other assays. *J Immunol Methods* 347:70–78. <https://doi.org/10.1016/j.jim.2009.06.008>
 19. Singh SK, Clarke ID, Hide T, Dirks PB (2004) Cancer stem cells in nervous system tumors. *Oncogene* 23:7267–7273. <https://doi.org/10.1038/sj.onc.1207946>
 20. Adamski V, Hempelmann A, Flüh C, Lucius R, Synowitz M, Hattermann K, Held-Feindt J (2017) Dormant glioblastoma cells acquire stem cell characteristics and are differentially affected by temozolomide and AT101 treatment. *Oncotarget* 8:108064–108078. <https://doi.org/10.18632/oncotarget.22514>
 21. Atkinson GP, Nozell SE, Benveniste ET (2010) NF-kappaB and STAT3 signaling in glioma: targets for future therapies. *Expert Rev Neurother* 10:575–586. <https://doi.org/10.1586/ern.10.21>
 22. Auffinger B, Tobias AL, Han Y, Lee G, Guo D, Dey M, Lesniak MS, Ahmed AU (2014) Conversion of differentiated cancer cells into cancer stem-like cells in a glioblastoma model after primary chemotherapy. *Cell Death Differ* 21:1119–1131. <https://doi.org/10.1038/cdd.2014.31>
 23. Stern R, Jedrzejewski MJ (2006) Hyaluronidases: their genomics, structures, and mechanisms of action. *Chem Rev* 106:818–839. <https://doi.org/10.1021/cr050247k>
 24. Kohno N, Ohnuma T, Truog P (1994) Effects of hyaluronidase on doxorubicin penetration into squamous carcinoma multicellular tumor spheroids and its cell lethality. *J Cancer Res Clin Oncol* 120:293–297
 25. Kerbel RS, St Croix B, Florenes VA, Rak J (1996) Induction and reversal of cell adhesion-dependent multicellular drug resistance in solid breast tumors. *Hum Cell* 9:257–264
 26. Baumgartner G, Gomar-Höess C, Sakr L, Ulsperger E, Wogritsch C (1998) The impact of extracellular matrix on the chemoresistance of solid tumors—experimental and clinical results of hyaluronidase as additive to cytostatic chemotherapy. *Cancer Lett* 131:85–99
 27. Whatcott CJ, Han H, Posner RG, Hostetter G, Von Hoff DD (2011) Targeting the tumor microenvironment in cancer: why hyaluronidase deserves a second look. *Cancer Discov* 1:291–296. <https://doi.org/10.1158/2159-8290.CD-11-0136>
 28. Chen J, Li Y, Yu TS, McKay RM, Burns DK, Kernie SG, Parada LF (2012) A restricted cell population propagates glioblastoma growth after chemotherapy. *Nature* 488:522–526. <https://doi.org/10.1038/nature11287>
 29. Gallego O (2015) Nonsurgical treatment of recurrent glioblastoma. *Curr Oncol* 22:e273–e281. <https://doi.org/10.3747/co.22.2436>
 30. Wang HH, Liao CC, Chow NH, Huang LL, Chuang JI, Wei KC, Shin JW (2017) Whether CD44 is an applicable marker for glioma stem cells. *Am J Transl Res* 9:4785–4806
 31. Harada H, Takahashi M (2007) CD44-dependent intracellular and extracellular catabolism of hyaluronic acid by hyaluronidase-1 and -2. *J Biol Chem* 282:5597–5607. <https://doi.org/10.1074/jbc.M608358200>
 32. Duterme C, Mertens-Strijthagen J, Tammi M, Flamion B (2009) Two novel functions of hyaluronidase-2 (Hyal2) are formation of the glycoalyx and control of CD44-ERM interactions. *J Biol Chem* 284:33495–33508. <https://doi.org/10.1074/jbc.M109.044362>
 33. Sironen RK, Tammi M, Tammi R, Auvinen PK, Anttila M, Kosma VM (2011) Hyaluronan in human malignancies. *Exp Cell Res* 317:383–391. <https://doi.org/10.1016/j.yexcr.2010.11.017>